Hindawi
International Journal of Polymer Science
Volume 2023, Article ID 9471371, 12 pages
https://doi.org/10.1155/2023/9471371

Research Article

Fabrication and Properties of Polycaprolactone/Poly(Butylene Succinate) Blends Based on Electrospinning

Lan Yu,[1] **Feng Wang**,[2] **and Shan Huang**[3]

[1]*Guangdong Polytechnic of Environmental Protection Engineering, Foshan 528216, China*
[2]*School of Chemistry and Chemical Engineering, South China University of Technology, Guangzhou 510640, China*
[3]*School of Biological and chemical Engineering, Changsha University, Changsha 410022, China*

Correspondence should be addressed to Lan Yu; joy99joy@163.com and Shan Huang; 879314@163.com

Received 1 October 2022; Revised 26 November 2022; Accepted 15 December 2022; Published 15 March 2023

Academic Editor: Maria Laura Di Lorenzo

Electrospinning technology is famous for its simple preparation, and accurate and easy control of process parameters. It is widely used in ultrafine filtration membrane and biological tissue engineering support. Polycaprolactone (PCL) and poly(butylene succinate) (PBS) have good biocompatibility and are commonly used materials in electrospinning. In this study, the relationship between the electrospun sample, process parameters, and spinning solution of PCL/PBS blend system was systematically studied in an electrospinning experiment. The morphology characteristics, thermodynamic properties, and microstructure of the electrospun sample were screened by scanning electron microscopy, thermogravimetric analysis, differential scanning calorimetry, and X-ray diffraction. The optimum conditions of electrospinning with high practical value were obtained.

1. Introduction

Polycaprolactone (PCL) is a synthetic, thermoplastic, incomplete crystallization polymer that has good biocompatibility, natural degradation, and safety. It is one of the most studied synthetic polymers in the field of biomedical materials and has been approved by the US Food and Drug Administration for its many advantages. PCL is used extensively because of its low glass transition temperature (−60°C) and high permeability [1]. PCL is widely used in tissue engineering and other fields because it neither cause hemolysis nor does it destroy and change platelets and ions in the body [2–5]. However, the mechanical strength and melting point of PCL are relatively low. The hydrophilicity of PCL is hindered by the presence of five repeated methylene units in the molecular structure, resulting in a slow degradation rate and a long degradation cycle. The degradation rate of PCL is usually adjusted by modifying PCL or adding more easily degradable materials to suit different types of requirements [6].

Poly(butylene succinate) (PBS) is a new type of polyester developed gradually. It is mainly obtained from the enzymatic treatment of aliphatic diols and their polycondensates as well as cellulose and reducing sugars and other reusable raw materials. In addition, it is a recyclable material [7–9]. PBS has similar tensile strength and elongation at break to polyethylene with melting point of 115°C, glass transformation temperature of −33°C, and decomposition temperature of about 350°C. PBS not only has low cost and high efficiency, lack of pollution to the ecological environment, and good biocompatibility, but also has excellent mechanical properties and good processing characteristics. Therefore, the application of PBS in biomaterials has attracted research attention at home and abroad [10, 11]. Sonseca et al. demonstrated the effectiveness of wet electrospinning for the fabrication of poly(butylene succinate-co-dilinoleic succinate) (PBS-DLS) fibers. The goal was for tissue engineering [8]. However, research on its application in biomedical field is still insufficient at present.

Electrospinning fibers are widely used in bioengineering. All human tissues and organs are made up of fibrous structures. For example, the periosteum tissue is made up of osteoblasts, collagen fibers, and stromal fluid; the skin contains

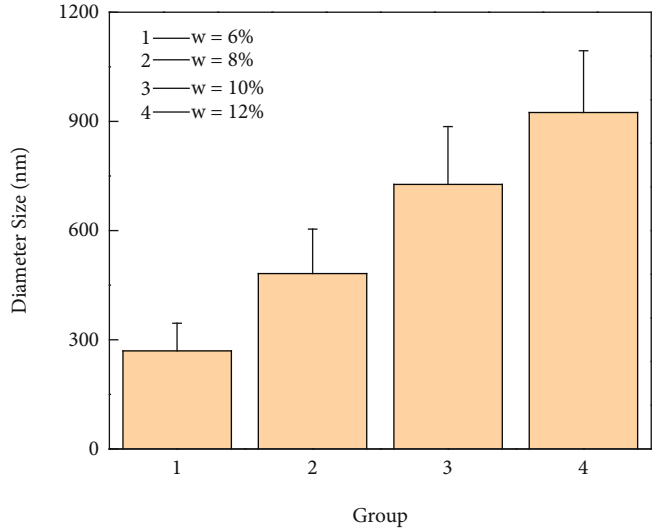

Figure 1: Relationship between electrospinning diameter and solution mass fraction.

collagen fibers and elastic fibers; and the cartilage contains tiny collagen fibers [12, 13]. These tissues and structures are made up of different nanofibers that are connected in different ways. In particular, they show great potential for tissue engineering and controlled drug delivery because they can mimic the structure of the extracellular matrix (ECM) and serve as models for cell growth and proliferation. Electrospinning is capable of fabricating fibers in the range of nanoscale. Electrospun fibers are also being examined as ECM-mimicking substrates in tissue engineering. [14, 15]. In recent years, one of the main research areas of electrospinning technology applied in tissue engineering is the use of biopolymers to produce biocompatible scaffolds for cell growth and reproduction, which can be used for various types of biological tissue repair. For example, PCL has good histocompatibility and can be fabricated into scaffolds by electrospinning for the healing of body [16–18]. Controlled release drug delivery systems can improve the therapeutic efficacy of drugs, reduce drug toxicity, and ensure the safety of drug delivery [19]. To control the drug release system with electrospinning, the choice of polymer carrier is very important because these polymers need to be biocompatible and have low repulsion to the human body. Therefore, fibers obtained by electrospinning can effectively improve the biocompatibility and degradation rate of the polymer.

With the rapid technological development, an increasing number of new materials have been developed, and electrospinning materials are one of the important ones [20–22]. The wide range of these materials in biological and medical uses makes them become increasingly important in the field of new materials. In this experiment, PCL and PBS were dissolved in hexafluoroisopropanol (HFIP) solutions to obtain high quality dope. By controlling the variable parameters, this study investigated various factors and process conditions that influenced the spinning product. Through careful analysis of various factors, we obtained a relatively complete electrospinning process and a relatively high quality electrospinning product that has important reference value for PCL/PBS blend to synthesize the best spinning product. The raw materials PCL and PBS used in this experiment have the characteristics of low price and environment friendliness, which are conducive to the concept of green chemistry and environmental protection chemistry.

2. Results

2.1. Influence of Mass Fraction on Diameter of Electrospinning. Electrospinning solution concentration has a huge impact. In the process of spinning a solution by a strong electrospinning field force, the solution surface tension is certain; as the voltage increases, the electrospinning field force will be greater than the liquid surface tension, and traction solution is present at the needle cone form of the so-called "Taylor cone," namely under the continuous high voltage. The solution will be pulled through the Taylor cone to spiral toward the flat plate receiver, and the solution jet is dispersed into multiple streams from the initial stream and finally hit the receiver panel. Different kinds of solutions have different voltages to form Taylor cones, and the solutions of the same solute have different voltages to form Taylor cones because of different concentrations. Figure 1 shows that with increasing solution concentration, in the case of other conditions unchanged (Table 1), the diameter of electrospun fiber is increasing when the solution concentration from 6 to 10%, from 269.8 to 727.2 nm in diameter. PBS-based copolymers containing dilinoleic acid/diol degrade into non-cytotoxic products and their properties can be modulated by varying the ratio of hard to soft segments covering a wide range of strength and elasticity.

For the same solution, the solution viscosity increases with concentration. In the spinning process, when the voltage is constant, that is, the electrospinning field force is constant, the higher the viscosity, the more spinning materials are contained in the thin flow dispersed by the solution jet, and the thicker the single spinning bundle is finally formed. When the concentration of the spinning solution continued

Table 1: Concentration of electrospinning solution.

Serial Number	Spinning fluid composition (mass ratio)	The mass fraction (%)	Spinning voltage (kV)	Push the note rate (mL/h)
1	PCL/PBS = 1 : 1	6	12	0.8
2	PCL/PBS = 1 : 1	8	12	0.8
3	PCL/PBS = 1 : 1	10	12	0.8
4	PCL/PBS = 1 : 1	12	12	0.8

to increase to 12%, a large number of spherical droplets appeared in the electrospun sample, the spinning diameter increased to 924.5 nm, and the spinning was very uneven [Figure 2(d)]. This was because when the concentration of the solution was too large, the existing voltage could not fully disperse the spinning jet, and the jet could not be directly drawn to the receiver before bunched. When the solution concentration is within the range of 8–10%, the spinning effect is better, with high density and moderate uniformity (Figures 2(b) and 2(c)). Therefore, subsequent experiments to explore other factors are carried out under the mass fraction of electrospinning solution of 10%.

2.2. Influence of Polymer Ratio on Diameter of Electrospinning. According to Figures 3 and 4, in the solution with the same concentration, the electrospinning diameter of the homopolymer solution is greatly affected by the two polymers, and the diameter of the polymer increases with increasing PCL ratio. The electrospinning diameter of pure PCL (i.e., PCL/PBS = 1 : 0) is the largest, reaching 750.1 nm (Figure 3(a)). The electrospinning diameter of pure PBS spinning solution (i.e., PCL/PBS = 0 : 1) is 577.9 nm [Figure 3(b)]. It is related to the physical and chemical properties of raw materials. The molecular weight (M_n) of PCL with 90,000 and the molecular weight (M_n) of polybutanediol succinate (PBS) with 10,000 are used in this experiment. The larger molecular weight of PCL makes its viscosity larger than that of polybutanediol butyrate, and the dispersion stream formed by the spinning jet containing PCL is relatively coarser under the action of the same electric field force. This conclusion can be applied to the actual production to adjust the diameter of spinning products of the two polymer spinning solution. In addition, we found that the spinning density of PCL was lower than that of PBS when other unrelated factors were the same, indicating that the spinnability of PCL was slightly worse but the spinning diameter was larger; moreover, the spinnability of PBS was better but the spinning diameter was smaller. When the solution was formed after the mixture of the two polymers was spun, the spinning characteristics of the two polymers can be neutralized and electrospinning fibers with moderate spinnability and suitable diameter can be obtained.

2.3. Influence of Spinning Voltage on Diameter of Electrospinning. Voltage is an important factor in electrospinning. When the solution is determined, the surface tension is identified. Changing the potential difference between the positive and negative poles can change the shape of the protrusion formed when the spinning fluid is ejected from the needle, the current carried by the spinning fluid jet, and the movement track when ejected, thereby affecting the spinning pattern. When the voltage is small and moderate, the solution will form a "Taylor cone" at the needle, and the spinning solution can move toward the receiver regularly under the traction of electric field force, forming spinning fiber with relatively uniform morphology [Figures 5(a), 5(b), and 5(c)]. As the voltage increases, the electric field force increases, and the traction of the spinning fluid jet becomes stronger and stronger. The jet is dispersed into more streams to maintain the spiral motion, which will reduce the diameter of the electrospun fibers. Figure 6 shows that the spinning diameter decreased slightly when the voltage increased from 12 to 20 kV, but it was not obvious on the whole. When the voltage is too high, the "Taylor cone" can no longer be formed at the needle because the strong electric field force is higher than the surface tension of the droplet; as such, the spinning liquid is directly pulled by the electric field force from the inside of the needle and thrown to the receiver. In the process of movement, it is no longer a scattered stream, but a small droplet directly attached to the panel. The observed microstructure is multi-sphere and spin-like fiber with fine diameter [Figure 5(d)]. High voltage also speeds up the movement rate of the solution in the needle and makes the solution splash, so there are electrospun samples outside the receiver panel under high voltage, causing a certain degree of corrosion to the equipment. The blending solution can form electrospun sample at 12–20 kV(25°C), and a large number of droplets will appear in the sample at a higher temperature.

2.4. Influence of Injection Rate on Diameter of Electrospinning. The pushing rate of spinning solution can also affect the formation of "Taylor cone" and its stability. As shown in Figure 7, when the pushing rate increases from 0.6 to 1.0 mL/h, the diameter of electrospinning also increases from 372.8 to 785.5 nm. Because the "Taylor cone" is relatively stable at this time, the gradually increasing spinning jet makes the voltage distribution more dispersed and carries less current per small flow. Therefore, the diameter of the electrospinning bundle also increases correspondingly [Figures 8(a), 8(b), and 8(c)]. Of course, this was done under the condition that the overall injection rate was low. When the injection rate was too high, the "Taylor cone" could not continue to exist stably due to excessive spinning jets, and a large number of droplets would appear on the spinning bundle [Figure 8(d)]. When the injection rate is too small, the solution supply rate cannot support the amount of solution required for spinning at the current voltage, and the solution in the needle may be intermittent; the extremely unstable outflow will increase the number of droplets in the electrospun sample [Figure 8(a)]. In addition, we found that when the solution pushing injection rate was too high, many branch spinning bundles with very fine diameters were added to the original spinning bundles, whose diameters were about 1/4–1/5 of the main spinning bundles. This

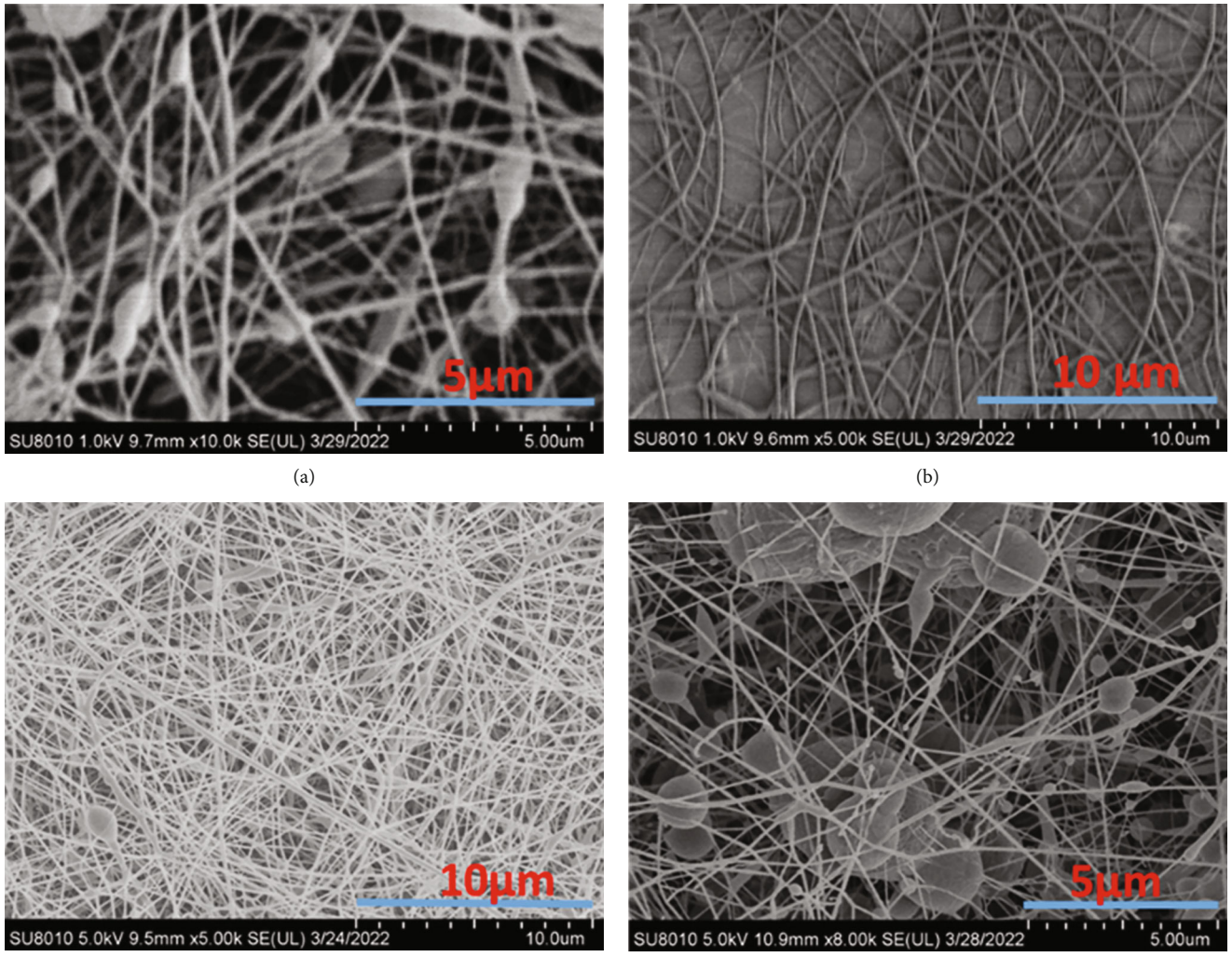

Figure 2: Scanning electron microscopy of electrospinning [mass fraction of spinning solution is different: (a) 6%; (b) 8%; (c) 10%; and (d) 12%].

finding could be attributed to the large volume of "Taylor cone" formed in the spinning process due to the high pushing injection rate and sufficient supply of spinning material. The primary dispersion flow is dispersed in the process of movement, forming a secondary dispersion flow, and finally the coexistence of primary and secondary spinning strands appears on the receiving panel.

2.5. Thermogravimetric Analysis of Samples. As shown in Figure 9, the decomposition stages of the five samples are basically the same, which can be roughly divided into two processes. In the initial condition, there will be certain mass fluctuations. The analysis samples are flake or strip, and the center of gravity position shifts after heating in the crucible, resulting in a slight change in weight. The second stage is the decomposition stage of PCL, PBS, and the blended silk products. According to Table 2, PBS has a low thermal decomposition temperature of 368°C and the maximum decomposition temperature of 394.7°C, whereas PCL has a high thermal decomposition temperature of 385.3°C and the maximum decomposition temperature of 407.6°C. The thermal decomposition temperature of electrospun sample formed by blending the two is related to the ratio. When PCL proportion is large, the thermal decomposition temperature of electrospun sample is correspondingly high; when the PBS proportion is large, the thermal decomposition temperature of theelectrospun sample is closer to PBS with lower decomposition temperature. When the proportion of PBS was increased from 20 to 80%, the thermal decomposition temperature of the spun sample decreased by 12.5°C. The lowest thermal decomposition temperature was 358.8°C when PCL/PBS = 1 : 1. By observing the thermal decomposition curve of polymer with different ratio, which indicates that the compatibility of PCL and PBS is good and no new substances are generated.

2.6. Differential Scanning Calorimetry of Samples. Melting temperature and crystallization were obtained by differential

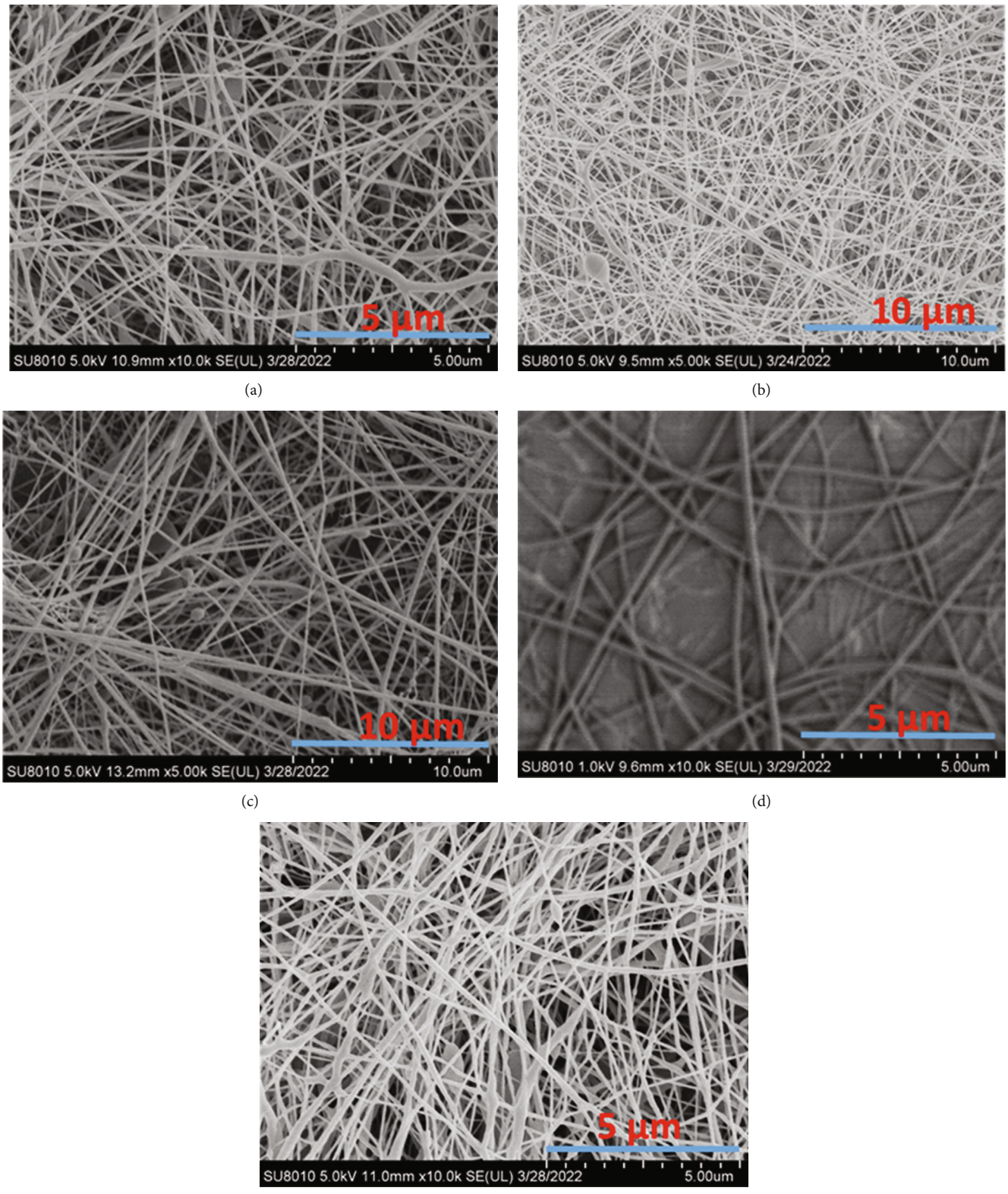

Figure 3: Scanning electron microscopy of electrospinning with different polymer ratios. (a) PCL/PBS = 1 : 4, (b) PCL/PBS = 1 : 1, (c) PCL/PBS = 4 : 1, (d) PCL/PBS = 1 : 0, and (e) PCL/PBS = 0 : 1.

scanning calorimetry (DSC). Figure 10 shows the DSC curves of the spun samples in different proportions. The melting temperature of PCL is 55.18°C, and that of PBS is 115.2°C. The thermal properties of the sample are slightly influenced by the ratio of electrospinning materials. Figure 10 showed DSC analysis of electrospun samples.

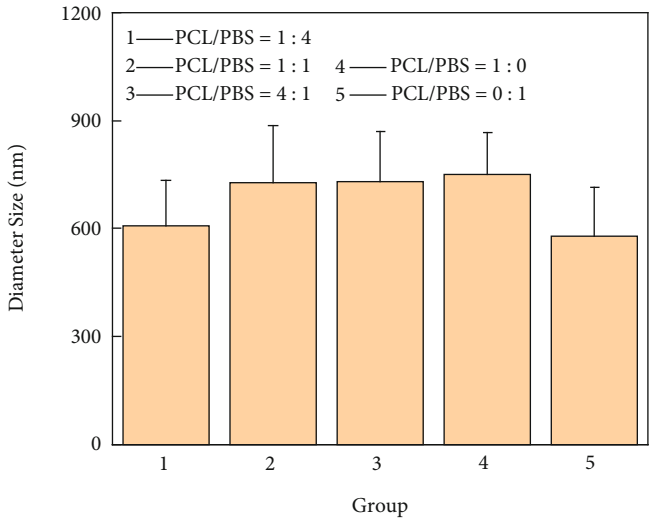

Figure 4: The relationship between electrospinning diameter and solution ratio.

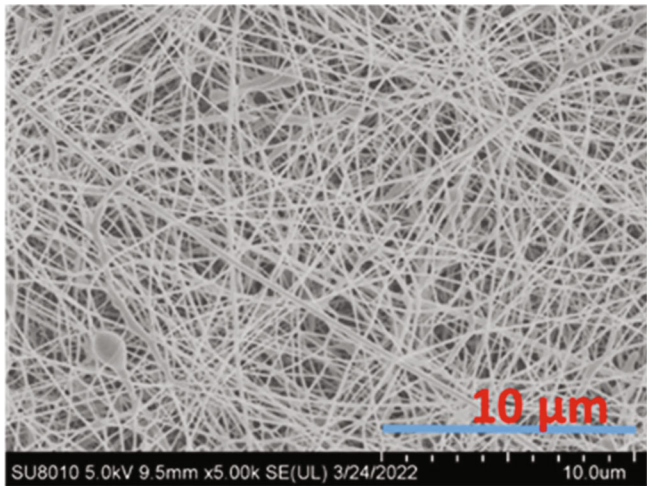

U = 12 kV

(a)

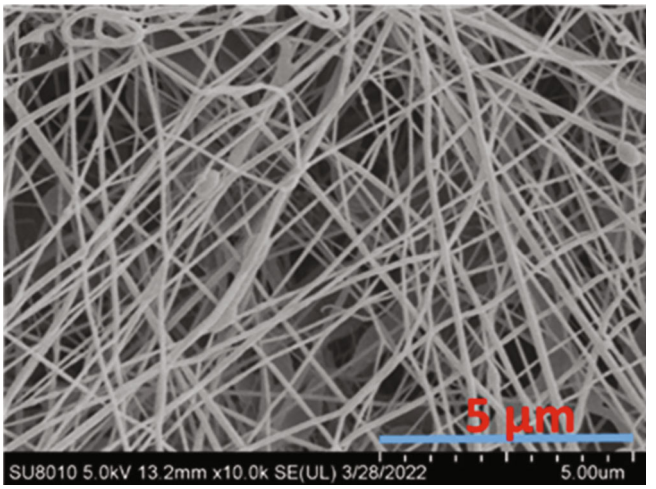

U = 16 kV

(b)

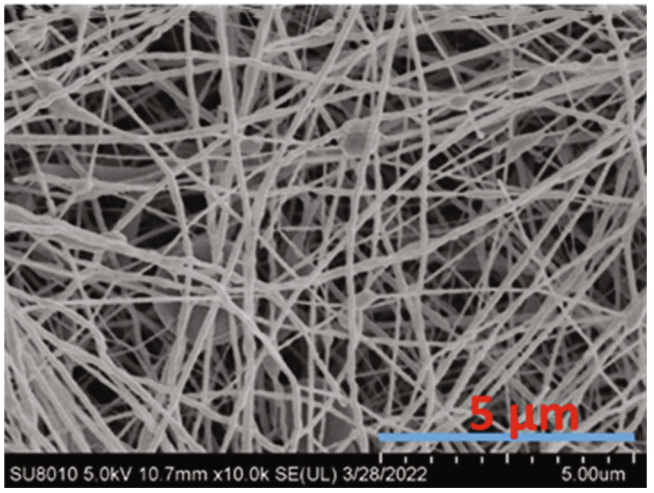

U = 20 kV

(c)

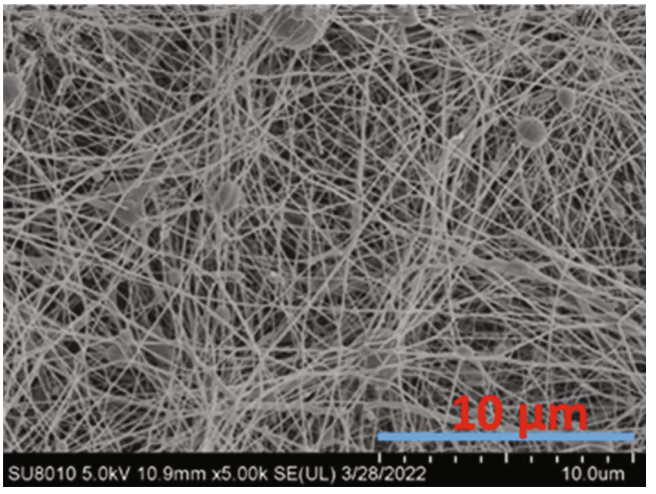

U = 24 kV

(d)

Figure 5: Scanning electron microscopy of electrospinning at different voltages. (a) 12 kV, (b) 16 kV, (c) 20 kV, and (d) 24 kV.

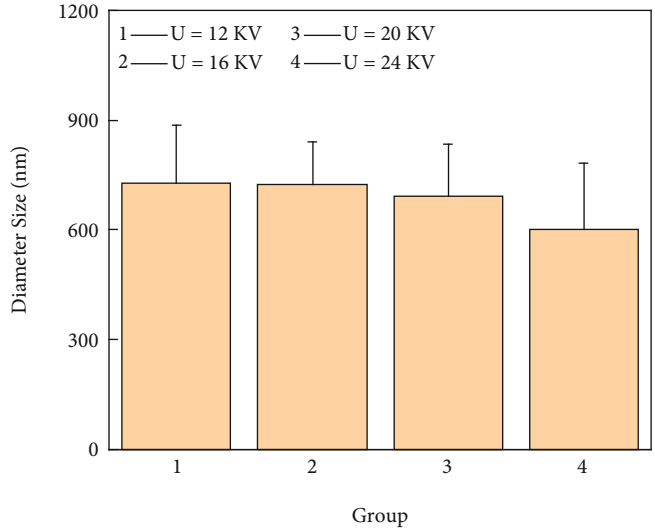

Figure 6: The relationship between electrospinning diameter and electrospinning voltage.

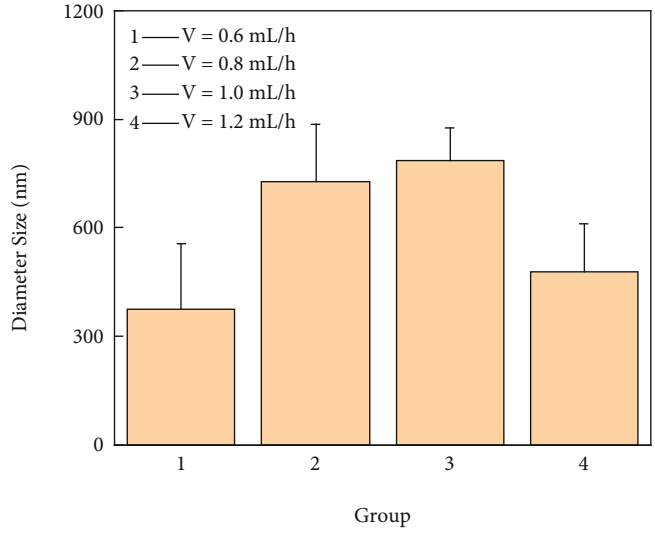

Figure 7: The relationship between electrospinning diameter and injection rate.

The thermal scanning was observed with the different ratio of PCL/PBS. Two melting endothermic peaks were observed, which correspond to the melting peaks of PCL and PBS, respectively. The higher temperature corresponds to the melting point of PBS, and the lower temperature corresponds to the melting point of PCL. No new melting peak was observed. They were incompatible in the crystal region; and therefore, exhibit their own melting points. With the increase of PBS, the peak with higher temperature gradually increased, whereas the peak with lower temperature gradually decreased. This phenomenon showed that the blend forms a heterogeneous system. The chains were wrapped around each other in the amorphous part. However, it was phase separation in the crystal region, which was microscopic. The moderate compatibility of the blends has greater practical value. The blends showed better properties than two kinds of components.

2.7. X-Ray Diffraction of Samples. X-ray diffraction (XRD) is used to describe the crystallization of the spun sample, analyze its crystallinity, and characterize its structure. As shown in Figure 11, the relationship between diffraction angle and peak intensity of the electrospun sample prepared after blending of the two polymers are almost the same. Several characteristic strong peaks are found at 21.06°, 23.38°, 19.38°, and 22.34°, which are in the same position as the measured strong peak of pure PCL and PBS. No new peak appears, indicating the lack of chemical reaction after the two polymers are mixed into a solution and spun under high pressure. As such, the spinning solution formed is uniform and stable and will not affect the crystallization of the filament.

2.8. Fourier Transform Infrared Spectra of Sample. The main Fourier transform infrared (FTIR) bands corresponding to

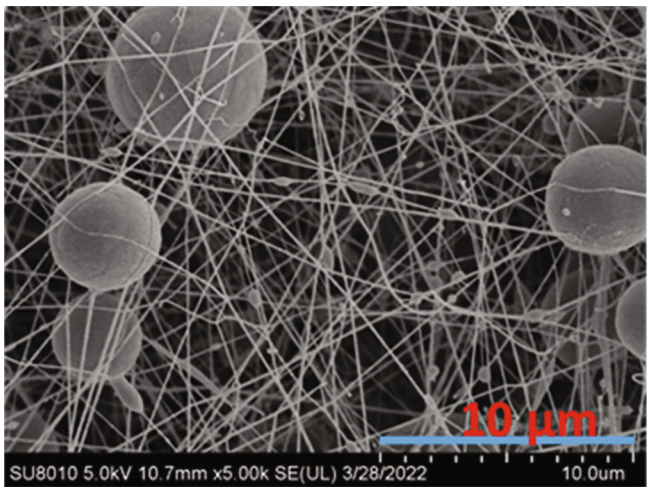

Injection rate = 0.6 mL h^{-1}

(a)

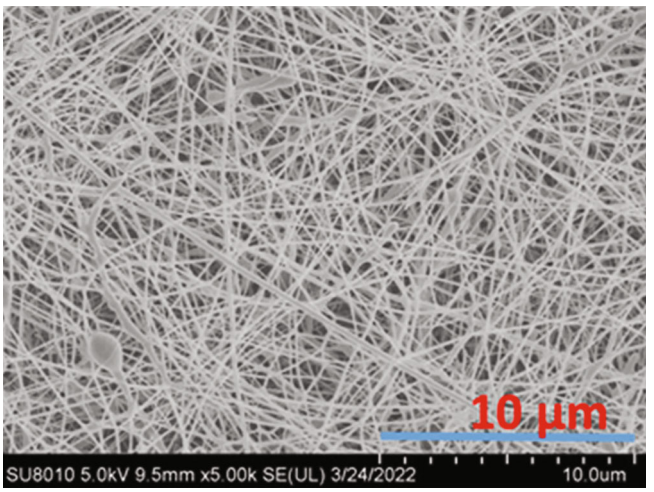

Injection rate = 0.8 mL h^{-1}

(b)

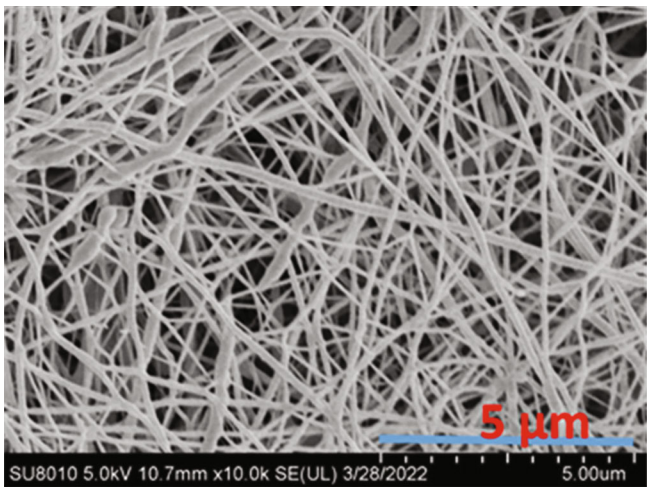

Injection rate = 1.0 mL h^{-1}

(c)

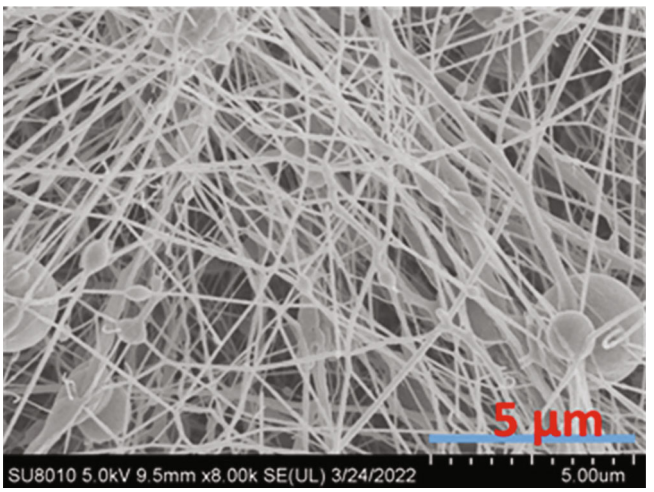

Injection rate = 1.2 mL h^{-1}

(d)

Figure 8: The relationship between electrospinning diameter and injection rate. (a) 0.6 mL h^{-1}, (b) 0.8 mL h^{-1}, (c) 1.0 mL h^{-1}, (d) 1.2 mL h^{-1}.

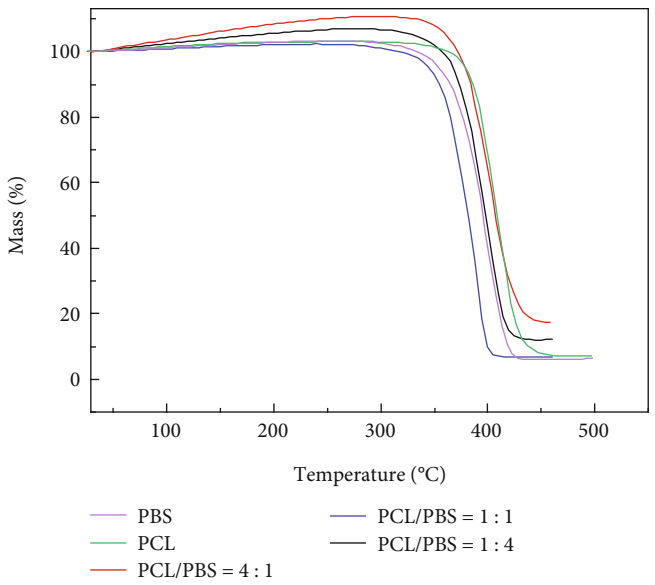

Figure 9: Thermogravimetric analysis of electrospun sample.

Table 2: Decomposition temperature of each sample.

Sample name	Thermal decomposition temperature (°C)	Maximum decomposition temperature (°C)
PBS	368.0	394.7
PCL	385.3	407.6
PCL/PBS = 4 : 1	379.7	385.1
PCL/PBS = 1 : 1	358.8	389.5
PCL/PBS = 1 : 4	366.6	371.6

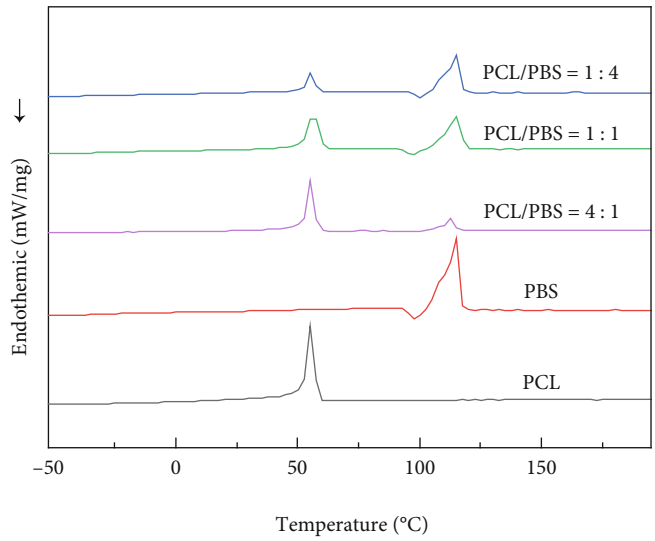

Figure 10: Differential scanning calorimetry analysis of electrospun samples.

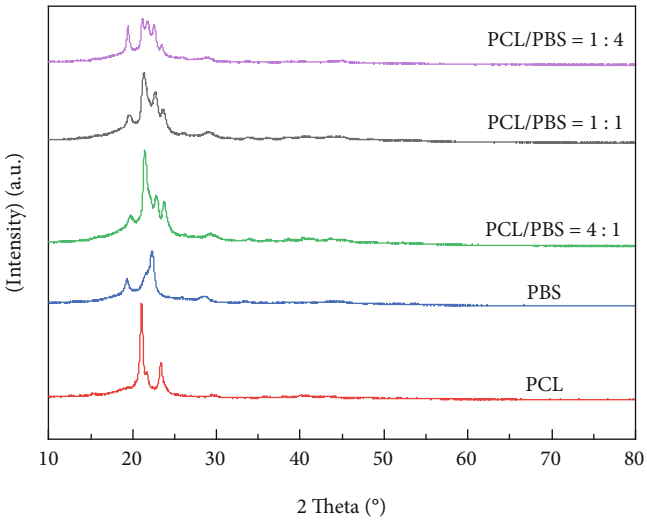

Figure 11: X-ray diffraction analysis of electrospun sample.

the individual polymers were identified. Figure 12 shows representative spectra. The regions that can be seen around 2948, 2861, 1726[1], and 1293 cm^{-1} are areas of PCL absorption. Spectra shows a $-CH_2-$ strtching band (2948 and 2861 cm^{-1}), C=O stretching band (1726 cm^{-1}), and $-(CH_2)_5-$ vibration absorption (at 1161 cm^{-1}) for PCL. In addition, the 1713 and 1161 cm^{-1} bands, assigned to the stretching band of C=O and vibration absorption band of C–O, respectively. The absorption peak of PBS and PCL were all presented in Figure 12. It was showed that there was no reaction between PBS and PCL. However, the peak height was changed with the mass fraction of PBS/PCL sample.

3. Materials and Methods

3.1. Materials. All solvents used in this study were purchased from Guangzhou Chemical Reagent Factory, Guangzhou, China. These chemicals were used as received without further purification.

3.2. Electrospinning. PCL/PBS solution at a concentration of 6, 8, and 10%, w/v was prepared at room temperature by dissolving the polymer in HIFP. The electrospinning was performed as follows: the electrospinning was equipped with a high voltage statitron (12 kV). The solution flow rate was 0.6, 0.8, 1.0, and 1.2 mL/h, and collecting distance was 10 cm at 25°C–28°C. The samples were dried in a vacuum oven for over 2 days to remove solvent residue for further application.

PCL/PBS was dissolved in HFIP as different mass ratio for 9 hours at room temperature. After its configuration stabilizes, the spinning solution is absorbed by the syringe and placed on the working table of the injection system. The injection block is moved to make it in contact with the syringe handle. The flat plate receiver is used to observe the spinning shape and effect at any time. The distance

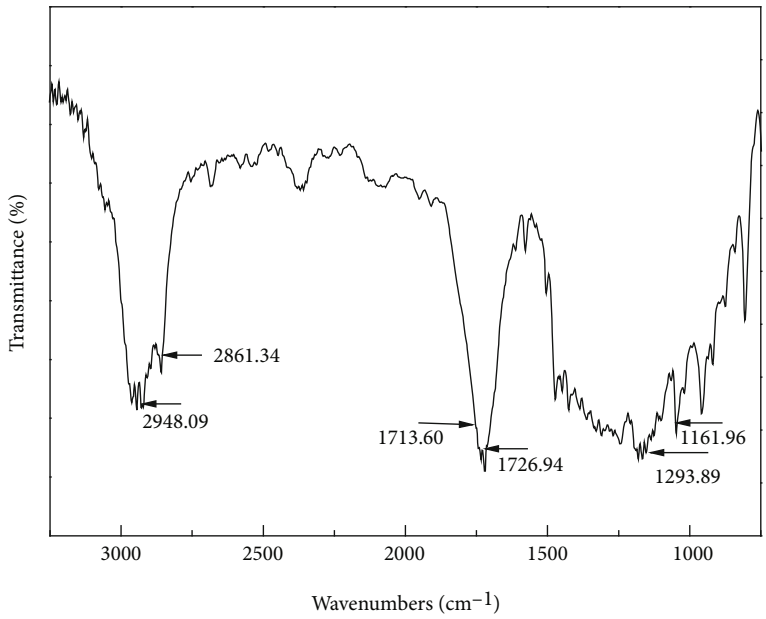

Figure 12: FTIR of electrospun sample.

between receiver and needle is adjusted to the appropriate position. Positive and negative high pressure contacts are clamped. Positive and negative high pressure contacts are started and adjusted to an appropriate value. The spinning solution is pulled to a cone under the action of high static power, forming a Taylor cone. Under the action of strong electric field, the jet is dispersed into multi-jet, which moves spirally to the receiver and accumulates on the surface, forming electrospinning. The spinning time of each spinning solution is 30 minutes. Control variable method was used in the spinning process to study the influence of spinning solution concentration, the ratio of two kinds of polymers at the same concentration, spinning voltage, and injection rate on the spinning results. SEM observation: The morphology of the electrospun sample was observed from the microstructure, and its diameter was measured by the ImageJ software.

3.2.1. Thermogravimetric Analysis. Thermal decomposition temperature was investigated using thermogravimetric analysis (TGA) 209 F1 purged with nitrogen. TGA was carried out over a temperature range from 35°C to 600°C at a scanning rate of 10°C minutes. The flow rate of gas was 20 mL/minutes.

3.2.2. Differential Scanning Calorimetry. The crystallization behavior of the polymers was investigated by modulated DSC (MDSC 2910, TA Instruments, DSC, MDSC 2910, TA Instruments Co., DE, USA) purged with nitrogen in cooling and heating process. DSC was carried out over a temperature range from 0°C to 200°C at a scanning rate of 10°C/minutes.

3.2.3. Scanning Electron Microscopy. The electrospun fibers of polymer were sputter coated with gold and visualized by scanning electron microscopy (SEM, JSM-6380LA Analytical SEM, JEOL Ltd., Tokyo, Japan) operated at an accelerating voltage of 15 kV. Fibers diameters were measured using the ImageJ software. At least 100 filaments of each sample from different SEM images were analyzed.

3.2.4. X-Ray Diffraction. The crystal structure of the samples was investigated by a Ultima IV X-ray powder diffractionmeter, Rigaku, Tokyo, Japan, using the Cu–Kα radiation (λ = 1.5406 Å and 40 kV, 40 mA).

3.2.5. Fourier Transform Infrared Spectroscopy. The sample was blended with potassium bromide (KBr) for FTIR spectroscopy (Nicolet/Nexus 670), and scanning absorption was recorded at wavenumber ranges in the range of 400–4000 cm^{-1} with a resolution of 4 cm^{-1}. FTIR spectrum of sample was detected in wavenumber ranges were compared with the reports.

4. Conclusion

The experiment used green and environment-friendly raw materials and had almost no by-products. In the whole experiment, the electrospinning process with PCL/PBS solution as raw material and its influencing factors were comprehensively analyzed based on experimental data analysis and relevant literature review. Solution mass fraction, polymer ratio, spinning voltage, and injection rate all affect the diameter of electrospinning, especially mass fraction. The most suitable mass fraction for spinning was 8–10%. The PCL/PBS blend solution was homogeneous and stable, and spinning products were obtained at various proportions. When PCL/PBS = 1 : 1, the spinning bundles were of high density and had uniform diameter. In a certain range, ideal electrospinning was obtained with slight difference in diameter between increasing and decreasing voltage. The optimal spinning voltage was 12–20 kV. When the voltage was too high, the droplets in the electrospun sample increased and

the diameter deviation was large. The pushing rate mainly affects the stability of "Taylor cone." If the pushing rate is too low, then the raw material supply will be insufficient and the spinning fluid will stop flowing. If the pushing rate is too high, then the spinning jet will disperse twice and form superfine filaments with no practical value and spherical filaments will appear.The spinning solution formed by PCL/PBS has good thermal stability and no chemical reaction or change of the crystallization of the electrospun sample when mixed in any proportion. It has high practical value. The solvent used in the experiment was hexafluoroisopropanol, instead of dichloromethane, which is relatively volatile, and toluene, which is more toxic, consistent with the concept of green chemistry and clean chemistry. This study provides a reference for the future development of PCL/PBS electrospinning. The product has regular appearance, good thermal stability, and strong practical value.

Data Availability

Data supporting this research article are available from the corresponding author or first author on reasonable request.

Conflicts of Interest

The author(s) declare(s) that they have no conflicts of interest.

Authors' Contributions

Lan Yu: conceptualization; Feng Wang: investigation; Shan Huang: writing—review and editing. All authors have read and agreed to the published version of the manuscript.

Acknowledgments

This work was supported by the Science Foundation of 2020 Foshan Self-funded Science and Technology Plan Project (Medical Science and Technology Research; Grant-No. 2020001005657), the Initial Funding of Scientific Research for the Introduction of Talents of Changsha University (Grant No. SF1814), and the Natural Science Foundation of Guangdong Province (Grant No. 2018A030313235).

References

[1] Z. Xiang, X. Guan, Z. Ma, Q. Shi, M. Panteleev, and F. I. Ataullakhanov, "Bioactive engineered scaffolds based on PCL-PEG-PCL and tumor cell-derived exosomes to minimize the foreign body reaction," *Biomaterials and Biosystems*, vol. 7, p. 100055, 2022.

[2] B. Sun, Z. Zhou, D. Li et al., "Polypyrrole-coated poly(l-lactic acid-co-ε-caprolactone)/silk fibroin nanofibrous nerve guidance conduit induced nerve regeneration in rat," *Materials Science and Engineering C*, vol. 94, pp. 190–199, 2019.

[3] D. Zhang, Z. Li, H. Shi et al., "Micropatterns and peptide gradient on the inner surface of a guidance conduit synergistically promotes nerve regeneration in vivo," *Bioactive Materials*, vol. 9, pp. 134–146, 2022.

[4] Y. M. Kang, S. H. Lee, J. Y. Lee et al., "A biodegradable, injectable, gel system based on MPEG-b-(PCL-ran-PLLA) diblock copolymers with an adjustable therapeutic window," *Biomaterials*, vol. 31, no. 9, pp. 2453–2460, 2010.

[5] R. Dorati, B. Conti, B. Colzani et al., "Ivermectin controlled release implants based on poly-D,L-lactide and poly-ε-caprolactone," *Journal of Drug Delivery Science and Technology*, vol. 46, pp. 101–110, 2018.

[6] N. He, L. Li, P. Wang, J. Zhang, J. Chen, and J. Zhao, "Dioxide/chitosan/poly(lactide-co-caprolactone) composite membrane with efficient cu(II) adsorption," *Colloids and Surfaces A: Physicochemical and Engineering Aspects*, vol. 580, p. 123687, 2019.

[7] H. Kim, M. S. Shin, H. Jeon et al., "Highly reinforced poly(butylene succinate) nanocomposites prepared from chitosan nanowhiskers by in-situ polymerization," *International Journal of Biological Macromolecules*, vol. 173, pp. 128–135, 2021.

[8] A. Sonseca, R. Sahay, K. Stepien et al., "Architectured helically coiled scaffolds from elastomeric poly(butylene succinate) (PBS) copolyester via wet electrospinning," *Materials Science and Engineering C*, vol. 108, article 110505, 2020.

[9] T. P. Gumede, A. S. Luyt, and A. J. Müller, "Review on PCL, PBS, and PCL/PBS blends containing carbon nanotubes," *Express Polymer Letters*, vol. 12, no. 6, pp. 505–529, 2018.

[10] W. J. Xie and X. M. Zhou, "Non-isothermal crystallization kinetics and characterization of biodegradable poly(butylene succinate-co-neopentyl glycol succinate) copolyesters," *Materials Science and Engineering C*, vol. 46, pp. 366–373, 2015.

[11] X. M. Zhou, "Synthesis and characterization of polyester copolymers based on poly(butylene succinate) and poly(ethylene glycol)," *Materials Science and Engineering C*, vol. 32, no. 8, pp. 2459–2463, 2012.

[12] C. Sanhueza, F. Acevedo, S. Rocha, P. Villegas, M. Seeger, and R. Navia, "Polyhydroxyalkanoates as biomaterial for electrospun scaffolds," *International Journal of Biological Macromolecules*, vol. 124, pp. 102–110, 2019.

[13] X. Ji, R. Li, W. Jia, G. Liu, Y. Luo, and Z. Cheng, "Co-axial fibers with Janus-structured sheaths by electrospinning release corn peptides for wound healing," *ACS Applied Bio Materials*, vol. 3, no. 9, pp. 6430–6438, 2020.

[14] X. Liu, Z. Ren, X. Meng, and Y. Xu, "Substrate topography regulates extracellular matrix component secretion by bone marrow-derived mesenchymal stem cells," *Journal of Science: Advanced Materials and Devices*, vol. 7, no. 2, p. 100437, 2022.

[15] S. Behtaj, F. Karamali, E. Masaeli, G. Y. Anissimov, and M. Rybachuk, "Electrospun PGS/PCL, PLLA/PCL, PLGA/PCL and pure PCL scaffolds for retinal progenitor cell cultivation," *Biochemical Engineering Journal*, vol. 166, p. 107846, 2021.

[16] K. L. Fujimoto, A. Yamawaki-Ogata, K. Uto, A. Usui, Y. Narita, and M. Ebara, "Long term efficacy and fate of a right ventricular outflow tract replacement using an elastomeric cardiac patch consisting of caprolactone and D,L-lactide copolymers," *Acta Biomaterialia*, vol. 123, pp. 222–229, 2021.

[17] E. S. Morokov, V. A. Demina, N. G. Sedush et al., "Noninvasive high-frequency acoustic microscopy for 3D visualization of microstructure and estimation of elastic properties during hydrolytic degradation of lactide and ε-caprolactone polymers," *Acta Biomaterialia*, vol. 109, pp. 61–72, 2020.

[18] W. Yang, G. Qi, H. Ding et al., "Biodegradable poly (lactic acid)-poly (ε-caprolactone)-nanolignin composite films with

excellent flexibility and UV barrier performance," *Composites Communications*, vol. 22, p. 100497, 2020.

[19] J. Zou, Y. Yang, Y. Liu, F. Chen, and X. Li, "Release kinetics and cellular profiles for bFGF-loaded electrospun fibers: effect of the conjugation density and molecular weight of heparin," *Polymer*, vol. 52, no. 15, pp. 3357–3367, 2011.

[20] M. Bao, X. Lou, Q. Zhou, W. Dong, H. Yuan, and Y. Zhang, "Electrospun biomimetic fibrous scaffold from shape memory polymer of PDLLA co-TMC for bone tissue engineering," *ACS Applied Materials and Interfaces*, vol. 6, no. 4, pp. 2611–2621, 2014.

[21] C. Wang, C. Y. Fang, and C. Y. Wang, "Electrospun poly(butylene terephthalate) fibers: entanglement density effect on fiber diameter and fiber nucleating ability towards isotactic polypropylene," *Polymer*, vol. 72, pp. 21–29, 2015.

[22] J. Zheng, G. Hua, J. Yu et al., "Post-electrospinning "Triclick" functionalization of degradable polymer nanofibers," *ACS Macro Letters*, vol. 4, no. 2, pp. 207–213, 2015.